

TABLE II. Measurements and data on the eight prongs of the P^- star shown in Fig. 2.

Track number	Range mm	Number of plates traversed	Dip angle	Projected angle	$p\beta$ Mev/c	Ionization g/g	Identity	E_{kin} Mev	Total energy Mev
1	0.59	2	-56.5°	103°			$p(?)$	10	18
2	27.9	11	$+6.5^\circ$	61.5°			π^-	43	183
3	>50	81	-73.5°	14.5°	250 ± 45	1.10 ± 0.04	$\pi(?)$	174 ± 40	314 ± 40
4	>14.2	16	$+53^\circ$	318.5°			$p(?)$	70 ± 5	78 ± 5
5	6.2	3	$+4^\circ$	305.5°			π^+	30 ± 6	170 ± 6
6	9.5	15	-63.5°	281°			$T(?)$	82	98
7	18.6	30	-83.5°	255°			π^-	34	174
8	>22.3	16	$+33^\circ$	163°	190 ± 30	~ 1	$\pi(?)$	125 ± 25	265 ± 25
								Total visible energy ^a :	1300 ± 50 Mev
								For momentum balance:	≥ 100 Mev
								Total energy release:	$\geq 1400 \pm 50$ Mev

^a To obtain the minimum possible value of the visible energy release, still consistent with our observations, one has to make the very unlikely assumptions about the identity of tracks 3, 6, 7, and 8: that tracks 3 and 8 are due to electrons, track 6 to a proton, and track 7 to a μ^- meson. The total visible energy release in this case becomes 1084 ± 55 Mev. To this must be added at least 50 Mev to balance momentum, bringing the total energy release to $\geq 1134 \pm 55$ Mev.

The observations do not allow us to rule out the possibility that tracks 3 and 8 are due to electrons. It is, however, very unlikely that a fast electron could travel 50 mm (1.7 radiation lengths) in the emulsion (as does track 3) without a great loss of energy due to bremsstrahlung. The energy (particle 3) deduced from the measured $p\beta$ ($E=250$ Mev) must be considered a lower limit.

In Table II, the pertinent data on the eight prongs are summarized. The last column gives the total visible energy per particle ($E_{kin}+8$ -Mev binding energy per nucleon, or $E_{kin}+140$ -Mev rest energy per π meson) for the most probable assignments as discussed above. The total visible energy is 1300 ± 50 Mev, and the momentum unbalance is 750 Mev/c. To balance momentum, an energy of at least 100 Mev is required in neutral particles (i.e., about 5 neutrons with parallel and equal momenta), which brings the lower limit for the observed energy release to 1400 ± 50 Mev.

However, as some of the identity assignments to the star prongs are not certain, we have also computed the energy release for the extreme and very unlikely assignments, given at the foot of Table II, which are chosen to give the minimum energy release. In this case the total visible energy is 1084 ± 55 Mev and the resultant momentum is 380 Mev/c, which to be balanced requires at least 50 Mev in neutral particles (three or four neutrons). In this unrealistic case the lower limit for the observed energy release is 1134 ± 55 Mev, which still exceeds the rest energy of the incoming particle by about three standard deviations.

We conclude that the observations made on this reaction constitute a conclusive proof that we are dealing with the antiparticle of the proton.

A second important observation is the high multiplicity of charged π mesons (one π^+ , two π^- , and two π mesons with unknown charge). The fact that so many π mesons escaped from the nucleus where the annihilation took place, together with the low number of heavy particles emitted (three), may indicate that the struck nucleus was one of the light nuclei of the emul-

sion (C, N, O). Two of the outgoing heavy prongs carried rather high energies (70 Mev for the proton, 82 Mev for the triton), and they may have resulted from the reabsorption of another two π mesons.

We are greatly indebted to the Bevatron crew for their assistance in carrying out the exposure. We also wish to thank Mr. J. E. Lannutti for help with measurements and the analysis of the event.

* This work was performed under the auspices of the U. S. Atomic Energy Commission.

¹ Chamberlain, Segrè, Wiegand, and Ypsilantis, Phys. Rev. **100**, 947 (1955).

² Chamberlain, Chupp, Goldhaber, Segrè, Wiegand, Amaldi, Baroni, Castagnoli, Franzinetti, and Manfredini, Phys. Rev. **101**, 909 (1956), and Nuovo cimento (to be published).

³ Chamberlain, Keller, Segrè, Steiner, Wiegand, and Ypsilantis, Phys. Rev. (to be published).

⁴ Several stacks exposed in the 700 Mev/c beam are being studied in Berkeley by A. G. Eksping and G. Goldhaber; W. W. Chupp and S. Goldhaber; R. Birge, D. H. Perkins, D. Stork, and L. van Rossum; W. Barkas, H. Heckman, and F. Smith; and in Rome by E. Amaldi, G. Baroni, C. Castagnoli, C. Franzinetti, and A. Manfredini.

⁵ Goldhaber, Goldsack, and Lannutti, University of California Radiation Laboratory Report UCRL-2928 (unpublished).

Lowest States of Particle Excitation in Even-Even Nuclei

R. THIEBERGER AND I. TALMI

Department of Physics, The Weizmann Institute of Science, Rehovoth, Israel

(Received March 7, 1956)

ENERGIES of first excited states in even-even nuclei plotted *versus* the neutron number lie on a rather smooth curve.¹ There are peaks at magic numbers and dips between them; in some of the valleys rotational levels occur, presumably of collective motion. At or near peaks there is evidence for the shell model interpretation of these $J=2$ states as due to particle excitation. This approach is particularly simple whenever there are only two nucleons outside (or missing

from) closed shells. In such a case it is possible to calculate the energy of the first excited state, provided some assumption on the nuclear forces and the radial wave functions is made. In the following we use harmonic oscillator wave functions and for simplicity choose the same value of the force constant throughout. We then try to see whether the 0—2 energy separation in all these cases can be obtained from the same charge-symmetric interaction with some form of the two-body potential.

We make the simplifying assumption of pure jj -coupling configurations (i.e., we neglect deviations from jj -coupling or any other configuration interaction). In some nuclei the configuration is uniquely assigned by the shell model. In the other cases we considered the few alternative configurations according to the shell model; from these we chose the one for which the result agrees with the definite cases. Supporting evidence for our assignments is found in the spins of neighboring odd-even nuclei. For example, such evidence shows that beyond 50 the protons fill the $g_{7/2}$ shell whereas the neutrons fill the $d_{5/2}$ shell; this agrees with our results for Ba^{138} and Zr^{92} . Our results indicate also a different order of filling for protons and neutrons beyond 28. This might be due to eight $f_{7/2}$ protons which strongly interact with $f_{5/2}$ neutrons in Ni^{58} , whereas in Zn^{68} there are also four $p_{3/2}$ neutrons.^{2,3}

The nuclei treated are listed in column 1 of Table I. Configuration assignments are given in column 2. In column 3 the experimental energies (in Mev) of the first excited states are given.⁴ In proton configurations there is an additional contribution of the Coulomb forces. This should be removed as we are interested only in the nuclear interaction. To do this we took the value of the energy parameter of the harmonic oscillator model to be $e^2(\nu/\pi)^{1/2} = 300$ kev which is reasonable for light nuclei.⁵ Changes of even 50 kev will change the results insignificantly as the electrostatic contribution is small compared to the actual energies. This

is clearly demonstrated in column 4 where the given data include the Coulomb correction.

Better agreement could be obtained by taking different values of ν for protons and neutrons. Even the same ν will yield different charge and mass distributions because of the different proton and neutron occupation numbers in heavier nuclei. Having a bigger ν_p further decreases the charge radius.⁶ A ratio $(\nu_p/\nu_n)^{1/2} = 1.07$ gives good results and was kept throughout. For a certain interaction, several values of $r_0\nu^{1/2}$ were examined (r_0 is the range of the forces). For each $r_0\nu^{1/2}$ a least squares fit was done to give the best value of the potential depth V . As the agreement for A^{38} (and S^{34}) was not good, they were excluded from the least squares fit. The approximate nature of our assumptions is seen from Ti^{50} and Fe^{64} (also from Ni^{58} and Ni^{64}). Although they are assigned complementary configurations, the energies are different. The final results show these differences to be quite regular: The first excited level for two nucleons is higher whereas for two holes is lower than the calculated values. Such differences limit the accuracy of our procedure.

With pure Wigner force very good agreement was obtained both for a Gaussian (column 5) and a Yukawa potential (column 6). Including Majorana force (the only independent central exchange interaction for identical nucleons), whose strength was treated as an additional parameter, did not make an improvement. For the best fit, the Majorana force strength was around 3% of that of the Wigner force. Moreover, the Serber interaction, $(1+P_x)V(r)$, for example, gave definitely worse agreement. This is rather unsatisfactory as considerable Majorana interaction is required for saturation. However, the situation is changed if tensor forces are also included. In a two-nucleon configuration, the tensor interaction has nonvanishing matrix elements only between triplet states; in these states, for identical nucleons, L is always odd. Thus the tensor interaction has effectively a factor $1-P_x$ and might cancel the

TABLE I. Comparison of experimental and calculated energy values (in Mev) of first excited states of some even-even nuclei.

Nucleus	Configuration	Exp. level	Exp. level with Coulomb corr.	Wigner force Gaussian potential $r_0\nu^{1/2} = 0.510$	Wigner force Yukawa potential $r_0\nu^{1/2} = 0.544$	Serber and tensor forces $r_0\nu^{1/2} = 0.544$
8O^{18}	$n d_{5/2}^2$	1.72	1.72	1.67	1.64	1.61
12Mg^{26}	$p d_{5/2}^2$	1.84	1.91	1.86	1.84	1.87
16S^{34}	$n d_{3/2}^2$	2.10	2.10	1.55	1.55	1.50
18A^{20}	$p d_{3/2}^2$	2.15	2.22	1.79	1.75	1.76
20Ca^{42}	$n f_{7/2}^2$	1.48	1.48	1.44	1.43	1.45
22Ti^{50}	$p f_{7/2}^2$	1.58	1.64	1.58	1.60	1.67
26Fe^{54}	$p f_{7/2}^2$	1.45	1.51	1.58	1.60	1.67
28Ni^{58}	$n f_{5/2}^2$	1.45	1.45	1.40	1.42	1.40
28Ni^{58}	$n f_{5/2}^2$	1.35	1.35	1.40	1.42	1.40
30Zn^{68}	$p (1p_{3/2})^2$	1.10	1.16	1.04	1.21	1.16
38Sr^{86}	$n g_{9/2}^2$	1.08	1.08	1.25	1.27	1.21
40Zr^{92}	$n (1d_{5/2})^2$	0.93	0.93	0.88	0.99	
50Sn^{122}	$n h_{11/2}^2$	1.14	1.14	1.11	1.14	
56Ba^{138}	$p g_{7/2}^2$	1.44	1.50	1.46	1.44	1.37
82Pb^{124}	$n (1f_{5/2})^2$	0.80	0.80	0.80	0.88	
84Po^{126}	$p h_{9/2}^2$	1.19	1.24	1.30	1.31	

TABLE II. Relation between the parameter $r_0\nu^{\frac{1}{2}}$ and the corresponding V for Wigner forces.

	Gaussian potential				Yukawa potential			
$r_0\nu^{\frac{1}{2}}$	0.6778	0.5942	0.4753	0.3962	0.6370	0.5439	0.5051	0.4159
V (Mev)	41.0	46.7	63.6	87.7	29.8	38.0	42.7	58.6
r_0 (10^{-13} cm)	2.01	1.76	1.41	1.17	1.88	1.61	1.49	1.23

contribution of Majorana forces. By adding tensor forces^{7,8} having the same Yukawa potential to the Serber mixture and taking into account the increased number of parameters, a much better agreement is obtained (results when known are presented in column 7). By using better values for the various ranges, the agreement could probably be improved.

The agreement is obtained for a rather wide range of $r_0\nu^{\frac{1}{2}}$. The relation between this parameter and the corresponding V is given, for Wigner forces, in Table II. The mean square deviation for all values listed is within 30% of the minimum value. To adjust the Pb²⁰⁸ charge radius to $1.0 \times A^{1/3} \times 10^{-13}$ cm, we take $\nu = 0.114 \times 10^{26}$ cm⁻² [$e^2(\nu/\pi)^{\frac{1}{2}} = 275$ kev]; the r_0 values given are obtained from this ν . The values of r_0 and V are fairly close to those derived from low-energy p - p and n - p scattering.⁹ It should be mentioned that p and higher-angular-momentum states of relative motion contribute considerably to the calculated results; this is manifested by the different results obtained with Wigner and Majorana forces.

No determination of the nuclear interaction is attempted here. Nevertheless, it is interesting to see the fair agreement obtained with the shell model calculations over a wide range of mass numbers, despite the crude assumptions and small number of parameters.

We would like to thank Dr. A. de-Shalit for helpful discussions.

¹ G. Scharff-Goldhaber, Phys. Rev. **90**, 587 (1953).

² A. de-Shalit and M. Goldhaber, Phys. Rev. **92**, 1211 (1953).

³ N. Zeldes, J. Nuclear Phys. (to be published).

⁴ Most of the data were communicated to us by G. Scharff-Goldhaber, to whom we would like to express our thanks.

⁵ B. C. Carlson and I. Talmi, Phys. Rev. **96**, 436 (1954).

⁶ M. H. Johnson and E. Teller, Phys. Rev. **93**, 357 (1954).

⁷ I. Talmi, Phys. Rev. **89**, 1065 (1953).

⁸ S. Eckstein, M.Sc. thesis, Jerusalem, 1955 (unpublished).

⁹ R. G. Sachs, *Nuclear Theory* (Addison-Wesley Press, Cambridge, 1953), pp. 34 and 153.

Polarization of Bremsstrahlen*

JOHN M. DUDLEY, FRED W. INMAN, AND ROBERT W. KENNEY

Radiation Laboratory, University of California,
Berkeley, California

(Received March 5, 1956)

RECENT work on the state of polarization of bremsstrahlung beams has been reported by several authors¹⁻⁴; the results of each paper are somewhat at variance with the others and with the theory.⁵⁻⁷

We have attempted to investigate this polarization effect, both because of interest in the phenomenon and because of possible application. In practically all the experiments on nuclear reactions an average has been taken over the possible states of polarization of the incident photons. It is apparent that if one were able to use polarized photons, additional information could be obtained.

In this work, the fractional polarization observed at angle θ in the laboratory system is defined by

$$P(\theta, E, k) = \frac{d\sigma_{\perp}(\theta, E, k) - d\sigma_{\parallel}(\theta, E, k)}{d\sigma_{\perp}(\theta, E, k) + d\sigma_{\parallel}(\theta, E, k)},$$

where $d\sigma_{\perp}(\theta, E, k)$ is the bremsstrahlung cross section per unit solid angle with the following parameters: The incident electron has energy E ; the energy of the emergent photon is in a band (defined below) about k ; and the electric vector is perpendicular to the plane containing the paths of the electron and the photon. Let $d\sigma_{\parallel}(\theta, E, k)$ be similarly defined for a photon with its electric vector parallel to the plane. The angle θ is shown in Fig. 1. Note that the value of polarization does not depend upon the azimuthal angle about the center of the bremsstrahlung beam, but the significance of $d\sigma_{\perp}$ and $d\sigma_{\parallel}$ does.

For the case in which the electron is relativistic both before and after the collision, the bremsstrahlen electric vectors are predicted to be predominantly in the angular range labeled " \perp " in Fig. 1. The calculations indicate that nearly the entire energy spectrum is partially polarized over a relatively large range of θ in the beam; however, the polarization is predicted to be

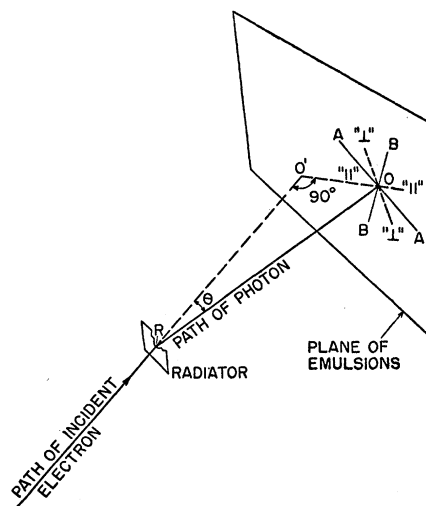


FIG. 1. Geometry of bremsstrahlung event and deuterium photoproton tracks. The intersection of the plane of emulsions, which is perpendicular to the path of the incident electron, with the plane of emission ($O'RO$) is along (OO'). The quadrants (AOB) in the plane of emulsions are centered on the two mutually perpendicular directions " \perp " and " \parallel ." RO' is the extended path of the incident electron.